Journal Pre-proofs

Fracture testing and estimation of critical loads in a PMMA-based dental material with nonlinear behavior in the presence of notches

A.R. Torabi, Sahel Shahbaz, S. Cicero, M.R. Ayatollahi

PII: S0167-8442(22)00035-0
DOI: https://doi.org/10.1016/j.tafmec.2022.103282
Reference: TAFMEC 103282

To appear in: *Theoretical and Applied Fracture Mechanics*

Received Date: 22 October 2021
Revised Date: 4 February 2022
Accepted Date: 8 February 2022

Please cite this article as: A.R. Torabi, S. Shahbaz, S. Cicero, M.R. Ayatollahi, Fracture testing and estimation of critical loads in a PMMA-based dental material with nonlinear behavior in the presence of notches, *Theoretical and Applied Fracture Mechanics* (2022), doi: https://doi.org/10.1016/j.tafmec.2022.103282

Fracture testing and estimation of critical loads in a PMMA-based dental material with nonlinear behavior in the presence of notches

A.R. Torabi [a,1], Sahel Shahbaz [b], S. Cicero [c], M.R. Ayatollahi[b]

[a] *Fracture Research Laboratory, Faculty of New Sciences and Technologies, University of Tehran, Tehran, Iran*

[b] *Fatigue and Fracture Research Laboratory, Center of Excellence in Experimental Solid Mechanics and Dynamics, School of Mechanical Engineering, Iran University of Science and Technology, Narmak 16846, Tehran, Iran*

[c] *LADICIM, Laboratory of Materials Science and Engineering, University of Cantabria, E.T.S. de Ingenieros de Caminos, Canales y Puertos, Av/Los Castros 44, Santander 39005, Spain*

Abstract

The goal of the present investigation is twofold: first, to provide new experimental data on the fracture behavior of biopolymer specimens containing notches, and second, to validate new fracture criteria to predict the corresponding experimental fracture loads. For this purpose, nine fracture experiments are conducted on U-notched rectangular specimens with different notch tip radii made of polymer-based dental material under monotonic tension. As the main outcomes of the experimental program, the fracture loads of the specimens, as well as the corresponding load-displacement curves, were recorded. Due to the nonlinear behavior of the dental material being tested, considerable plastic deformations are developed in the U-notch vicinity and, hence, the use of linear elastic notch fracture mechanics (LENFM) criteria (e.g., the maximum tangential stress (MTS) and mean stress (MS) criteria) for fracture (critical) load predictions provides inaccurate results. Consequently, the Equivalent Material Concept (EMC), which equates the nonlinear biopolymer material with a virtual brittle material having perfectly linear elastic behavior, is combined with the MTS and the MS criteria, allowing the use of LENFM for fracture load predictions of the U-notched biopolymer specimens being tested. It is observed that the two resulting criteria, EMC-MTS and EMC-MS,

[1]Corresponding author (A.R. Torabi). Tel.: +98 21 61115775; E-mail address: a_torabi@ut.ac.ir

provide very good predictions of the experimental results. From the viewpoint of mechanical design, the EMC-MTS criterion may be preferred to the EMC-MS criterion, given its inherent simplicity.

Keywords: dental material; notch fracture toughness; nonlinear behavior; Equivalent Material Concept (EMC); U-notch

Nomenclature

d_c	Critical distance in MS criterion
E	Elastic modulus
K_{IC}	Fracture toughness
P	Tensile load applied to the notched sample
P_c	Critical load
r_c	Critical distance in MTS criterion
σ_f^*	Tensile strength of the equivalent material
$\sigma_{\theta\theta}$	Tangential stress
σ_u	Ultimate tensile strength

1. Introduction

The fracture behavior of engineering components is one the main determining factors in structural design. Depending on the design requirements of the structure, notch-type defects of various shapes may be introduced in the structure. The initiation and propagation of cracks due to the stress concentration caused by notches may lead to catastrophic failures. Thus, the assessment of notches on the fracture behavior is of great importance.

Polymers may exhibit brittle, quasi-brittle, or ductile behaviors under different loading conditions, depending on their structure. In brittle and quasi-brittle polymers, cracks grow rapidly and fracture occurs abruptly. Concerning notches, due to their resulting stress concentration and the corresponding decrease of the load-carrying capacity (LCC), the prediction of fracture (critical) loads is important in the design of notched polymer components.

Dental materials are a group of biopolymers with structures very similar to bone cement structure. They consist of two main parts including, powder (polymethyl methacrylate) and liquid (methyl methacrylate) with almost the same weight percentage. The difference could be considered as the presence of extra additions such as antibiotics. Bone cement is utilized in clinical applications to stabilize articular prostheses in hip and knee joints. For example, in the case of hip implants, which are employed when the hip joint or the hip bone are catastrophically damaged, first, the damaged joint is removed, and then, the implant is inserted inside the resulting cavity. Finally, the cement is cast around it for fixing. The oldest and the most well-known group of bone cements are those based on polymeric materials, especially PMMA. These cements are mainly composed of a solid polymer powder (polymethyl-methacrylate) and a liquid monomer (methyl-methacrylate) [1].

The first successful use of this type of cement was made by Charnley [2] to stabilize the femoral head in 1970, which was the starting point for a lot of research and various surgical techniques. Saha et al. [3] comprehensively studied the mechanical properties of bone cement, including static properties (tensile, compressive, shear, and bending strengths), viscoelastic behavior (creep, stress relaxation, and effects of strain rate on mechanical properties), dynamic behavior (fatigue and impact), fracture toughness, and rheology [3]. Saha et al. [3] also analyzed some parameters affecting the mechanical properties, including the method of preparation, antibiotic inclusion, environmental conditions, irradiation, temperature, porosity, density, hardness, etc [3]. Juszczyk et al. [4] examined the properties of a commercial bone cement (CEMEX RX), such as the fatigue strength, the fatigue crack propagation resistance, and the fracture toughness. They reported an average value of fracture toughness (K_{IC}) of 1.38 MPa.$m^{0.5}$. Khandaker et al. [5] studied the elastic properties (Young's modulus and Poisson's ratio) and fracture toughness (K_{IC}) of PMMA and PMMA with micro and nano MgO particles cements. The results proved that the combination of micro and nano MgO particles with PMMA enhances the quality of the bone cement union. May-Pat et al. [6] studied the fracture behavior of acrylic bone cement modified with comonomers containing amine groups. Double-edge-notched tension (DENT) specimens were used in their study to determine the fracture toughness of the bone cement samples [6]. Zor et al. [7] studied the effects of residual stresses on the fracture energy of cement–bone and cement–implant prostheses. In order to compare the values of the fracture energy for bone and cement with the values of the interfacial fracture energy for cement (PMMA)/implant (316L) and cement/bone, K_{IC} and J_{IC} values of the bone and cement were determined experimentally [7].

In another study, Freitag et al. [8] investigated the characteristics of acrylic bone cements, mainly focusing on the fracture toughness and the fatigue behavior of two types of cold-cure bone cements, including Zimmer and Simplex-P. Robinson et al. [9] studied the PMMA type

bone cement. In order to evaluate the compressive strength and the fracture toughness, they utilized low viscosity PMMA, graphite-reinforced PMMA, and graphite-reinforced low viscosity PMMA. The result was that reinforcement of bone cement with graphite improves the fracture toughness of the cement by 32%. The influence of size-independent parameters and boundary conditions on the tensile strength, the fracture energy, and the characteristic length of wedge-splitting samples were studied by Merta et al. [10] Lewis et al. [11] proposed a method for determining the impact resistance of acrylic bone cements and assessed the relationship between the impact resistance and the fracture toughness. May-Pat et al. [12] investigated the effects of the incorporation of comonomers containing amine groups on the mechanical and fracture properties of acrylic bone cements. The results indicated that, on increasing comonomer content, both the strength and the elastic modulus decrease in bending and compressive tests. Also, it was proved that the fracture toughness (K_{IC}) and the critical strain energy release rate (G_{IC}) increase on raising the co-monomer concentration [12]. Ayatollahi et al. [13] investigated the effects of nano-hydroxyapatite (HA) on the mixed mode I/II fracture toughness of acrylic bone cements. For this purpose, semi-circular samples of PMMA cement with different amounts of HA powder in the cement matrix were prepared. It was found that adding up to 10 wt% HA into the cement causes an increase in the fracture toughness of PMMA/HA nano-composite in all fracture modes. Also, it was found that the generalized maximum tangential stress (GMTS) criterion could estimate the experimental results satisfactorily [13].

Gomez and Elices [14] estimated the fracture loads of brittle components with blunt V-shaped notches using the cohesive zone model (CZM). Due to the absence of singularity, linear elastic fracture mechanics (LEFM) could not predict the fracture load of these components. The concept of the critical stress intensity factor for sharp V-notches was extended to blunt V-notches under certain conditions, and a dimensionless fracture criterion

was proposed [14]. By utilizing the UMTS criterion, Ayatollahi and Torabi [15] predicted the fracture toughness and fracture initiation angle in U-notched Brazilian disk specimens with various notch tip radii under pure mode II loading. Also, Ayatollahi and Torabi [16, 17] applied the UMTS [16] and RV-MTS [17] fracture criteria to PMMA samples and, by proposing the fracture limit curves in terms of the notch stress intensity factors (NSIFs), they could successfully predict the fracture toughness of the notched samples under mixed mode I/II loading. Gomez et al. [18] assessed the fracture loads in U-notched PMMA samples under mixed mode I/II loading, experimentally and numerically using the cohesive zone model (CZM). Zhou et al. [19] studied the fracture behavior of Brazilian disk samples made of PMMA under quasi-static mode I loading. They measured the fracture toughness and analyzed the effects of the notch shape and length [19]. Bura and Seweryn [20] studied the fracture of unnotched, U-notched and V-notched PMMA samples under pure mode I loading. They evaluated the critical loads, the fracture initiation point, and the fracture initiation angle using both experimental and numerical methods [20]. Furthermore, the stress and strain distributions associated with the critical loads were presented using the finite element (FE) method.

In another study, Ayatollahi et al. [21] assessed the brittle fracture behavior of cracked semi-disk samples made of PMMA under three-point bending. The fracture load and the crack growth direction were experimentally recorded. It was shown that the fracture toughness of semi-circular bending (SCB) samples was overestimated by conventional mixed mode fracture criteria, such as the maximum tangential stress (MTS) criterion. The crack growth path predicted by the generalized MTS (GMTS) criterion was also shown to be in good agreement with the fracture path observed experimentally. Moreover, brittle fracture of SCB samples with V-shaped notches made of PMMA was assessed experimentally and theoretically under mode I loading for different notch geometries [22]. Torabi et al. [23]

studied the fracture of ductile polymeric samples with U-notches under tension. In order to predict the failure loads, the Equivalent Material Concept (EMC) combined with the mean stress (MS) and maximum tangential stress (MTS) criteria was utilized. It was shown that both EMC-MTS and EMC-MS criteria could predict the test results accurately without the need for elastic-plastic analyses of the polymeric samples.

As one of the most recent studies on the fracture of biomedical materials, Akbardoost et al. [24] investigated the effects of specimen size on the fracture resistance of bone materials by testing single edge notched bending (SENB) specimens and using a classical fracture criterion, called the modified maximum tangential stress (MMTS) criterion. It was revealed that the MMTS criterion could successfully predict the fracture resistance of the cracked bone by taking into account the effects of specimen size [24].

Regarding the existence of notches in polymeric bone cements, many examples can be mentioned. For instance, notches of various features form in the cement after drying as a result of taking the shape of the implant. In other words, depending on the implant geometry, some notches with different shapes are introduced in the bone cement. Due to the stress concentration at the notch neighborhood and the presence of the external loads transferred from the implant to the cement, crack(s) may initiate from the notch tip in the cement and propagate, leading to the failure of the cement and a necessary surgery for its replacement. Consequently, before using bone cements in biomedical applications, their notch resistance should be examined experimentally and/or theoretically.

One of the most important studies on the bone cement fracture was carried out by Taylor et al. [25] in 2004. First, they prepared test samples made of PMMA bone cement with central U-shaped notches and then they performed fracture tests at room temperature under pure mode I loading, from which the fracture loads of the samples were recorded. Finally, the

Theory of Critical Distances (TCD) was used to estimate the experimentally obtained fracture loads [25].

In this work, the aim is to investigate the fracture behavior of polymeric dental material weakened by U-notches with different tip radii under mode I loading in the presence of significant plasticity around the notch. To the authors' knowledge, there are no previous works analyzing dental material U-notched specimens subjected to tensile loads. The Equivalent Material Concept (EMC) and the MTS and MS criteria will be combined to predict the fracture loads of the dental material notched samples, with the aim of proving the capacity of both the EMC-MTS and the EMC-MS criteria to predict the experimental critical loads in this nonlinear material.

2. Experiments

2.1. Sample preparation

A PMMA (polymethyl methacrylate)-based dental polymer is used in this experimental campaign. It contains two main components including powder (polymethyl methacrylate) and liquid (methyl methacrylate). This type of material is commonly used as dental prostheses and partial dentures having normal curing time, low water absorption, high mechanical strength, good adhesion, and simple surface finishing. Polylactic acid molds were made using a 3D printer. Due to the need for machining and sizing of the specimens, the mold dimensions were 1 mm larger than the nominal size. Then, the dental material was prepared. To make the dental material, the powder and the liquid were mixed with the ratio of 4 to 3, respectively. There are two common methods for making the bone cements and dental materials: the first method is manual, in which the liquid and the powder are mixed at 23 °C for 60 seconds; in the second method, known as vacuum mixing, the powder and the liquid

enter the mixing chamber, with the pressure set to 0.7 bar. The mixture is kept in the chamber at 23 °C for 60 seconds. The vacuum mixing method was utilized in this research because it greatly reduces the porosity of the final product. The material was connected to the vacuum pump for 60 seconds and the mixture was stirred between the seconds 15 and 45 [26]. Figure 1 illustrates the time required to prepare a dental material sample. In fact, due to the elimination of bubbles caused by the mixing process, the material is connected to the vacuum pump. This is necessary because if bubbles exist in the mixture, the samples may break at lower critical loads. As soon as the one-minute process finished, the material was cast in the molds and kept at room temperature for 15 minutes to complete the curing process (see Figure 1). After that, samples were removed from the mold. In this sense, although lubricants and separators are applied to the mold surfaces, the material was not removed from the mold at the first step, given that Dacron fabrics were stuck to the mold floor and walls and, next, the dental material was poured into the molds. Because of the presence of Dacron fabrics, the dental material was easily removed from the molds. In Figure 2, the preparation steps of the material and the notched samples are shown.

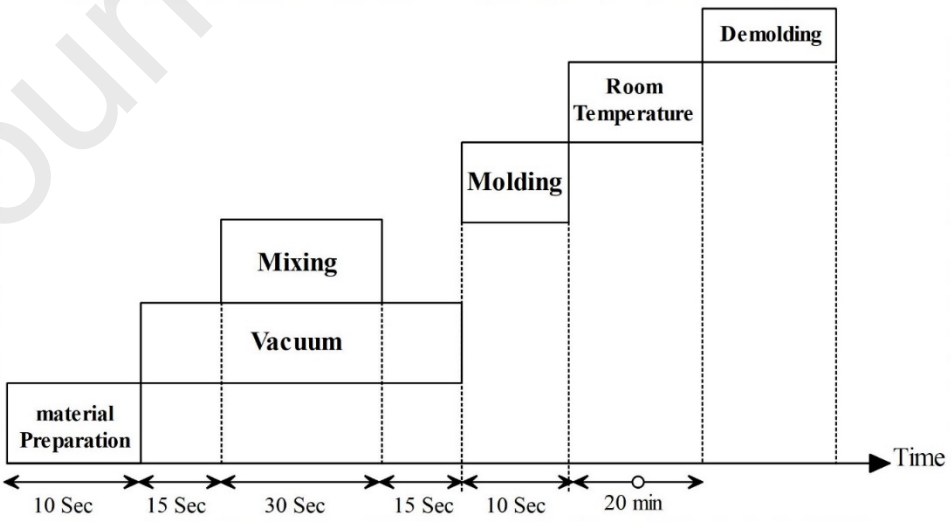

Fig. 1. Time required to prepare the dental material samples.

Fig. 2. Preparing the dental material and the test samples: (a) the dental material components (b) the vacuum pump machine (c) the molds made by the 3D printing method (d) the sample not separated from the mold (e) use of the Dacron fabrics (f) the samples after separating from the molds (g) after sizing the samples (h) after machining to create the desired notches (i) the broken samples and the fracture paths.

2.2. Samples geometry and testing

Fracture experiments were performed on rectangular samples with a central bean-like slot with two U-shaped ends, as shown in Figure 3a. The thickness of the samples was 3 mm, and the length of the bean-shaped slot was 10 mm. Table 1 reports the properties of the powder utilized to make the samples. Also, three different notch tip radii were considered: 1 mm, 2 mm, and 4 mm. After de-molding of the specimens, the rough surfaces were machined to obtain the nominal sizes. Moreover, the notches were generated by means of CNC machining

(see Figure 2). Before performing the main tests of the experimental program on the notched specimens, fracture and tensile characterization tests were also completed. Concerning the fracture tests, they were performed on three-point bending specimens to determine the (pure mode I) fracture toughness of the dental material (see Figure 3b). The length of the cracks was 8 mm, while their tip radius was about 25 μm, obtained from sharpening by means of a razor blade. First, a notch with the width of 0.3 mm and length of slightly less than 8 mm was introduced to the specimen. Then, the pre-existing notch was sharpened by a razor blade of 50 μm thick to have finally a pre-existing sharp crack of 8 mm long. Therefore, by involving the razor blade in the crack preparation process, it could be claimed that the pre-cracks in the specimens were sufficiently sharp, producing the crack tip stress singularity.

Figure 4 shows examples of the pre- and post-fracture U-notched samples, as well as the fracture characterization (cracked) samples before and during the fracture tests. As regards the tensile tests, ASTM-D638-IV [27] was utilized for fabricating the specimens (see Figure 3c) and determining the resulting tensile properties of the dental material. The specimens were subjected to tension and the values of the resulting engineering tensile stresses were calculated by dividing the loads by the initial cross-sectional area. The digital image correlation (DIC) method was used to obtain the strains accurately. The mechanical properties of the dental material tested are gathered in Table 2. Note that a 0.2% offset proof stress is considered herein as the yield strength of the material. This percent offset is common for many engineering materials like metals and plastics. In addition, the tensile testing and the DIC method are illustrated in Figure 5. Figure 6 represents both the true and the engineering stress-strain curves of the dental material. Note that in order to have quasi-static loading conditions, the test speed was constant and fixed at 0.5 mm/min. Moreover, for all the different specimens (un-notched, notched, or cracked) were fabricated and tested with a view to ensuring the repeatability of the tests.

Table 1. Characteristics of the powder and liquid used in the sample preparation.

Material	Characteristics	Supplier
Dental polymer	Powder: polymethyl-methacrylate Liquid: methyl-methacrylate monomer	Acropars pharmaceutical industry, Iran

Table 2. Main mechanical properties of the dental material being tested.

Material property	Value
Elastic modulus, E (GPa)	2.82 (±0.16)*
Poisson's ratio, ν	0.31 (±0.02)
Ultimate tensile strength, σ_u (MPa)	48.73 (±0.72)
Yield strength, σ_y (MPa)	34.68 (±0.58)
Fracture toughness, K_{IC} (MPa.m$^{0.5}$)	1.32 (±0.08)

*Values of standard deviation in parenthesis

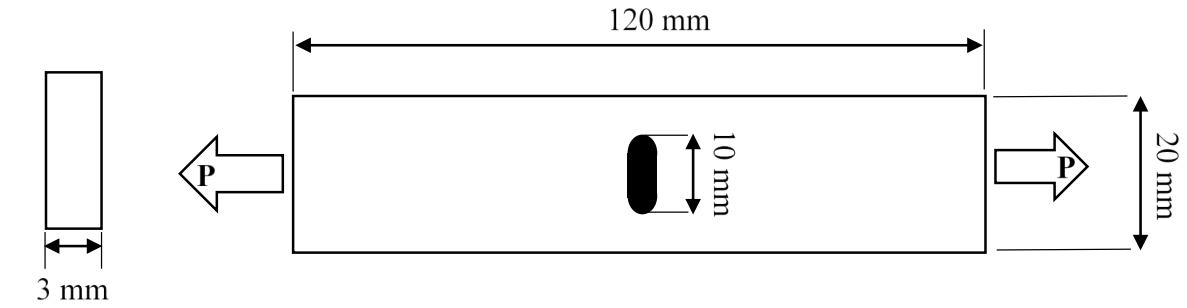

(a)

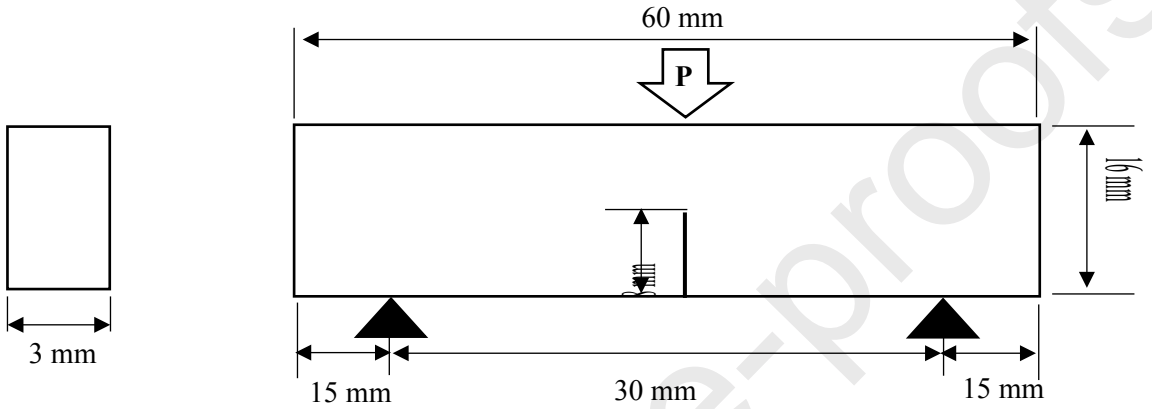

(b)

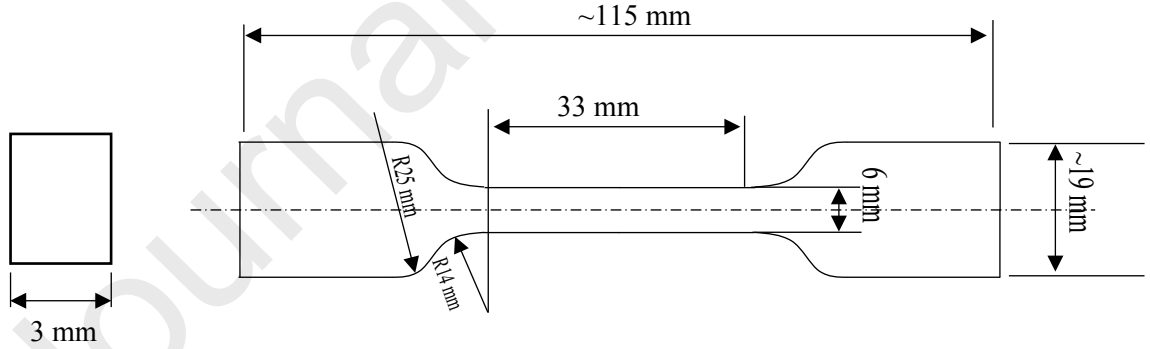

(c)

Fig. 3. Dimensions of the samples tested: (a) U-notched samples, (b) cracked samples, (c) standard tensile test samples.

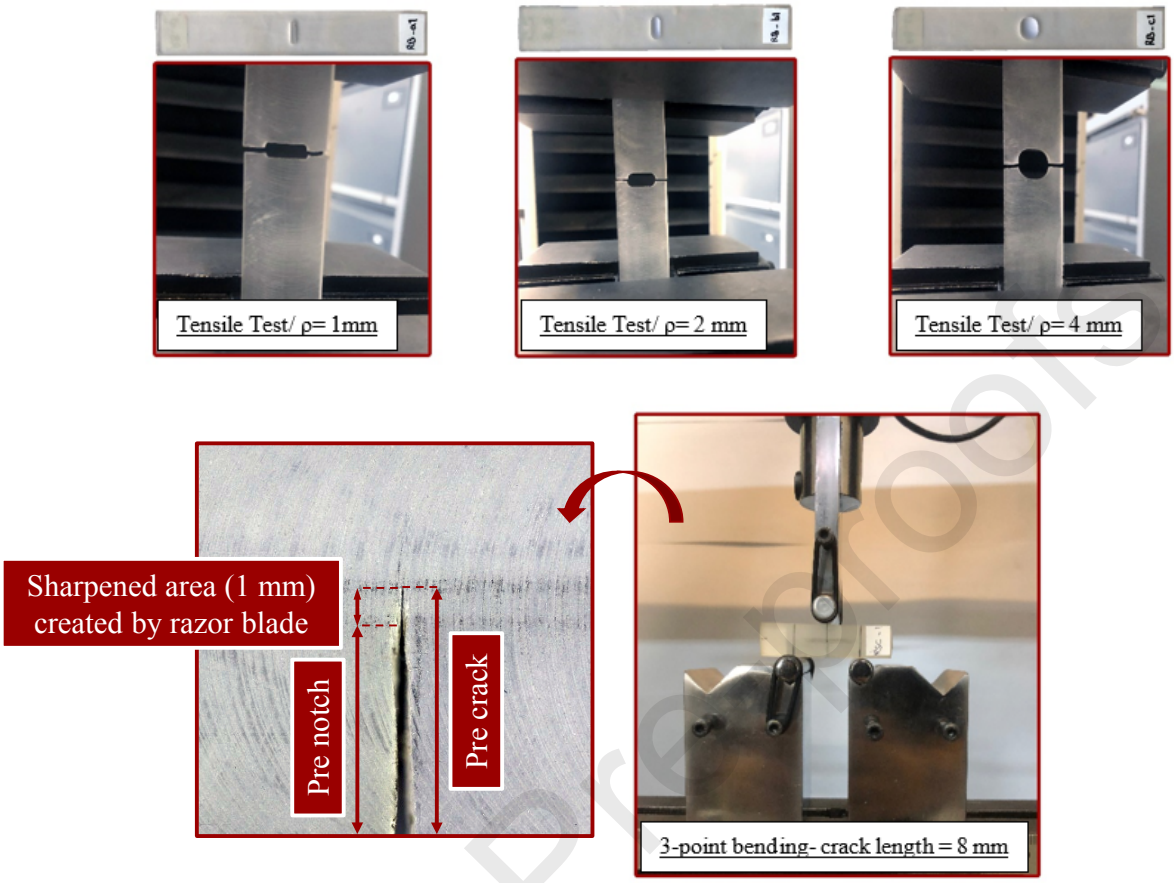

Fig. 4. Notched (top) and cracked (down) specimens, before and after the fracture tests.

Fig. 5. Un-notched specimen inside the tensile testing machine and the DIC method.

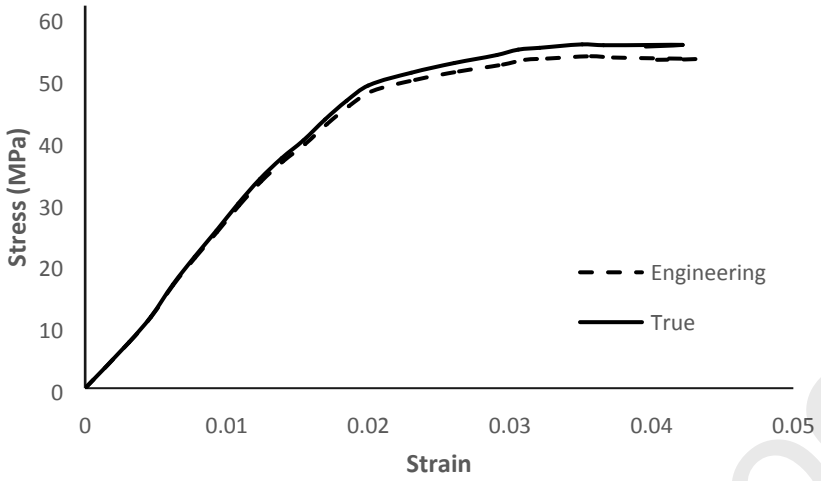

Fig. 6. Tensile stress-strain curves of the dental material.

Tables 3 and 4 summarize the fracture loads of the U-notched and the cracked specimens, respectively. It should be underlined that in some cases, data scattering was rather large due to molding process. In that situation, the samples were fabricated and tested up to 8 times to exclude irrational data. However, in general, the standard tensile tests, fracture toughness tests, and notch fracture toughness tests were all repeated three times to check the repeatability of the results. Note that P_i (i=1, 2, 3) denotes the fracture loads for the three replicas, while P_m specifies the mean values of the three fracture loads. Also, the specimen index in Tables 3 and 4 is generally defined in the form of X-N, in which X denotes T (tensile) or B (bending) and N denotes the notch tip radius (1, 2, 4 mm) or the crack length (8 mm).

Table 3. Fracture loads of the U-notched rectangular dental material samples.

Specimen index	P_1 (N)	P_2 (N)	P_3 (N)	P_m (N)
T-1	840	900	930	890
T-2	950	990	1120	1020
T-4	970	1035	1095	1030

Table 4. Fracture loads of the cracked dental material samples.

Specimen index	P_1 (N)	P_2 (N)	P_3 (N)	P_m (N)
B-8	144	150	141	145

Figure 7 displays an example of the load-displacement curve for the U-notched samples with 1 mm notch tip radius. It can be observed how the behavior of the curve is noticeably nonlinear, indicating the presence of significant plastic deformations in the vicinity of the notch at the moment of crack initiation from the notch tip.

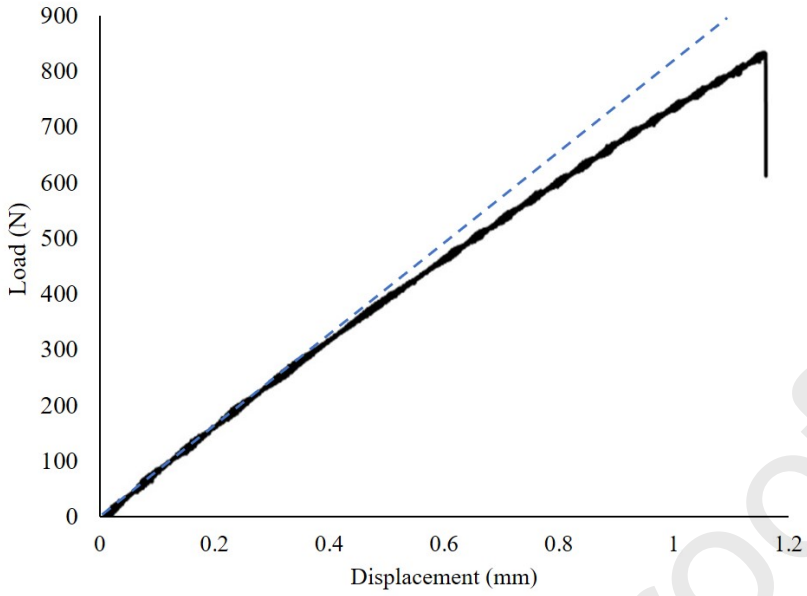

Fig. 7. Load-displacement curve for a U-notched sample with 1 mm notch tip radius (T-1), corresponding to the first replica (i=1, P_1).

3. Combined fracture criteria

This section provides a brief explanation of both the Equivalent Material Concept (EMC) and the classical criteria of the maximum tangential stress (MTS) and the mean stress (MS), which are basically related to the prediction of (critical) fracture loads in brittle materials. By combining the MTS and the MS with the EMC, the fracture loads of the U-notched dental material samples (with nonlinear behavior) will be predicted here.

3.1. The Equivalent Material Concept

The Equivalent Material Concept (EMC) was first proposed by Torabi [28] By implementing the EMC, a material developing a ductile tensile stress-strain curve and having K-based fracture toughness is equated with a virtual brittle material having the same fracture toughness and elastic modulus, but different tensile strength. In order to obtain the tensile strength of the equivalent material, it is assumed that the strain energy density (SED), i.e., the

area under the tensile stress-strain curve, required to initiate the necking in the real ductile material, is equal to the SED needed for sudden fracture in the virtual brittle material. Under this hypothesis, instead of analyzing a ductile material with elastic-plastic behavior, one can study a virtual brittle material with linear-elastic behavior. Thus, by applying the EMC, it is possible to use brittle fracture criteria to predict ultimate failure in materials with ductile tensile behavior [28], as is the case for the dental material analyzed here.

Figure 8a schematically shows the tensile stress-strain curve of a typical ductile material. The hatched area identifies the SED absorbed by the ductile material prior to the necking. As stated in the EMC definition, the equivalent brittle material has the same elastic modulus and fracture toughness as the real ductile material, but its tensile strength (σ_f^*) is different from the strength of the ductile material. Figure 8b illustrates the stress-strain curve of a typical brittle material. The tensile strength of the equivalent material is calculated by assuming the SED value of the equivalent material (i.e., the gray area in Figure 8b) to be the same as that of the real ductile material. The gray area under the curve of the equivalent brittle material is simply equal to 1/2 $\sigma_f^* \times \varepsilon_f^*$, which can be rewritten as ${\sigma_f^*}^2/2E$. Accordingly, the following equation can be used to calculate the tensile strength of the equivalent material (σ_f^*), in which E and $(SED)_D$ are the elastic modulus and the SED for the ductile material until necking, respectively.

$$(SED)_D = \frac{{\sigma_f^*}^2}{2E} \rightarrow \sigma_f^* = \sqrt{2E(SED)_D} \quad (1)$$

Once the tensile strength of the equivalent brittle material has been derived, it is possible to apply brittle fracture criteria to predict the fracture behavior (i.e., critical loads) of notched ductile components.

In the next subsections, the maximum tangential stress (MTS) and the mean stress (MS) criteria are briefly explained. Also, by combining the MTS and the MS criteria with the EMC

(leading to the EMC-MTS and the EMC-MS criteria, respectively), the fracture loads of the tested U-notched dental material specimens will be theoretically predicted, and compared with the experimental ones.

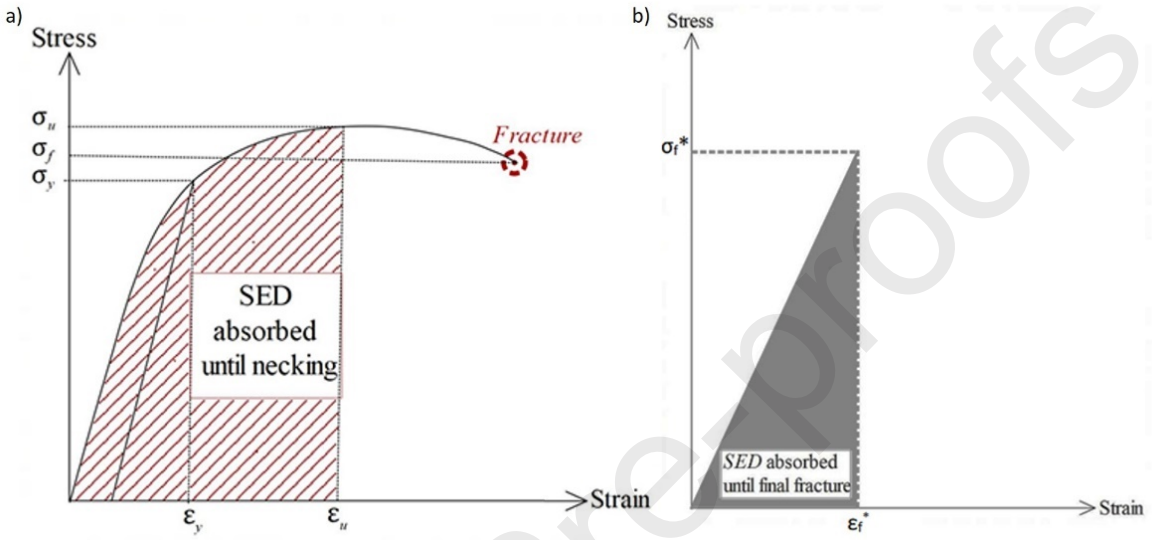

Fig. 8. a) Schematic of the engineering tensile stress-stain curve for a ductile material. σ_y: yield stress; σ_u: ultimate tensile strength; σ_f: stress at rupture and b) Schematic of the tensile stress -strain curve of the equivalent material.

3.2. Maximum tangential stress criterion

The maximum tangential stress (MTS) criterion was first proposed by Erdogan and Sih [29] in 1963. This criterion has been frequently used to predict the brittle failure of engineering structures containing sharp cracks. In 2009 and 2010, this criterion was extended by Ayatollahi and Torabi [16, 17] from sharp cracks to V- and U-shaped notches.

According to the maximum tangential stress (MTS) criterion, fracture in a brittle member occurs when the tangential stress ($\sigma_{\theta\theta}$) reaches the material critical stress (σ_c) at a specific critical distance from the notch tip (r_c). In this criterion, both the critical stress and the critical

distance are assumed to be material properties, both being independent of the loading conditions and the geometry of the notched samples. The value of the critical distance can be obtained from equation (2) [16], in which the parameter K_{IC} denotes the fracture toughness of material. Moreover, the critical stress for the brittle and quasi-brittle materials is usually assumed to be equal to the ultimate tensile strength of material, σ_u [30-32]. However, it should be noted that in some publications, the critical stress of material has been obtained to be 3-5 times larger than the uniaxial strength to get prediction close to the experiments [33-35]. The difference between the tensile strength and critical stress for a material depends mainly on the level of ductility of material.

$$r_c = \frac{1}{2\pi}\left(\frac{K_{IC}}{\sigma_c}\right)^2 \tag{2}$$

As mentioned in Section 1, a modified version of the MTS criterion, namely the modified maximum tangential stress (MMTS) criterion, has been recently proposed and utilized by Akbardoost et al. [24] for predicting the fracture resistance of bone materials by taking into account the effects of specimen size.

3.3. Mean stress criterion

In accordance with the mean stress (MS) criterion, fracture in brittle components takes place when the average value of tangential stress ($\sigma_{\theta\theta}$) over a specified critical distance from the notch tip (d_c) attains the critical stress (σ_c). Like r_c, the critical distance d_c is also assumed to be a material property. The expression of d_c is also presented in equation (3) [36].

$$d_c = 4r_c = \frac{2}{\pi}\left(\frac{K_{IC}}{\sigma_c}\right)^2 \tag{3}$$

4. Finite element analysis

The U-notched dental material samples with 1, 2, and 4 mm notch tip radii were simulated by using the finite element (FE) code ABAQUS 6.14, with the aim of obtaining the linear-elastic stress distributions in the vicinity of the notch tips. For meshing the samples, eight-node plane-stress quadratic elements were used. To demonstrate the convergence of the numerical results, several analyses with different numbers of elements were performed. The mesh sensitivity analysis was performed and, accordingly, the size of the elements near the notch was fixed at 0.02 mm. The mesh pattern of one of the U-notched specimens is depicted in Figure 9. The fine mesh pattern at the notch tip shown in Figure 9 is a consequence of the significant stress gradient.

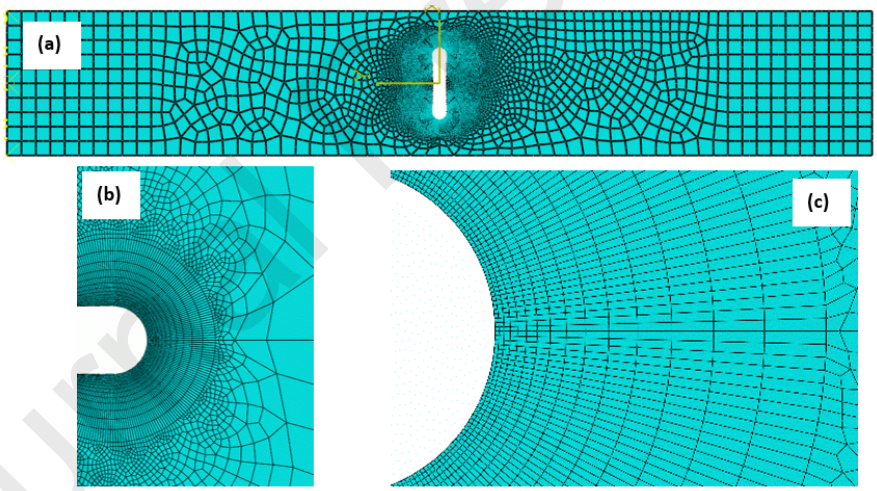

Fig. 9. A sample mesh pattern for the U-notched dental material specimens: (a) whole specimen (b) vicinity of the notch (c) notch tip with high magnification.

Figure 10 represents the elastic tangential stress contours around a U-shaped notch with the tip radius of 1 mm (values are in MPa). The symmetry of the butterfly wings around the notch tips can be observed, confirming the pure mode I loading on the U-notched dental material samples.

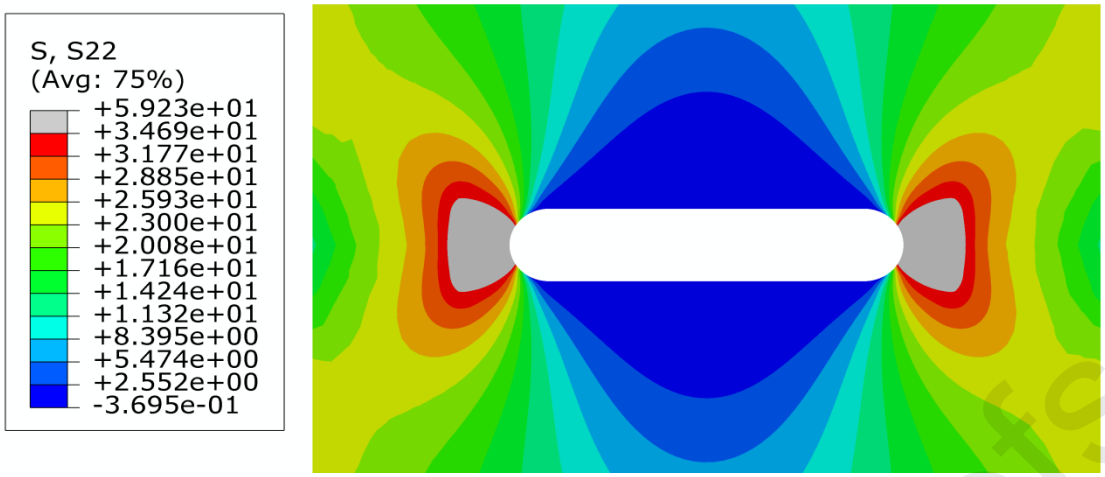

Fig. 10. Distribution of the elastic tangential stress contours formed near the U-shaped notch with 1 mm tip radius.

Likewise, in order to determine the fracture toughness of the dental material, it is necessary to simulate the cracked samples under three-point bending (TPB) loading in the FE software. Figure 11 shows a schematic of the cracked sample meshed in the FE software. In order to obtain highly precise numerical results, very small collapsed singular elements are used in the vicinity of the crack tip. Note that a mesh-sensitivity analysis is performed herein to determine the appropriate size of elements at the crack tip neighborhood. By modeling the cracked sample in the FE software, the number of J-integral contours evaluated (typically 5 contours) is kept constant and the mesh size is changed. It is found that for the mesh sizes smaller than 0.02 mm, the values of converged J-integrals are almost the same and hence, this mesh size is finally selected for numerical analysis.

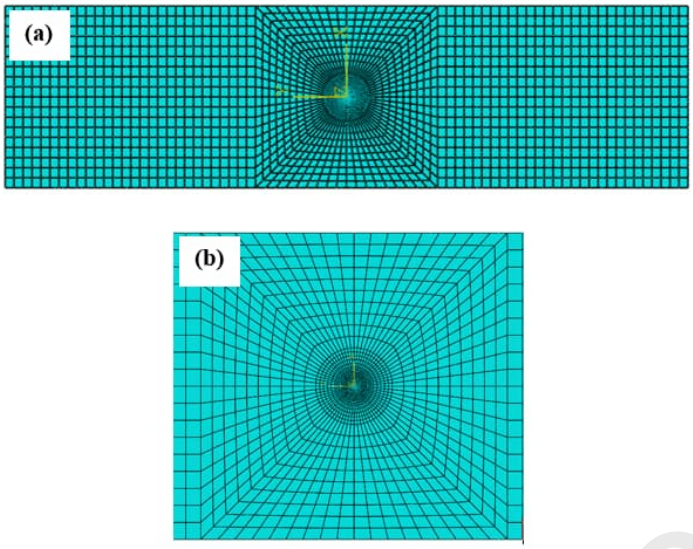

Fig. 11. The mesh pattern applied to the cracked FE model: (a) whole specimen (b) vicinity of the crack tip.

The FE model of the TPB cracked specimens was subjected to the average fracture load obtained from the experiments (i.e., 145 N in Table 4), obtaining the corresponding mode I stress intensity factor (K_I) from the linear elastic solution. Given that the load applied to the model is equal to the sample fracture load, the obtained K_I value is equal to the fracture toughness (K_{IC}) of the dental material, this being 1.32 MPa.m$^{0.5}$.

Figure 12 shows an example of the load-displacement curve obtained in the cracked dental material specimens. It is evident that the curve is linear up to final fracture, suggesting that the specimen fails within the small-scale yielding (SSY) regime. In order to take into account the effect of the small plastic zone around the crack tip on the material fracture behavior, it is modified herein by means of the virtual crack extension method (VCEM), reported in [37]. According to the VCEM, the radius of the plastic zone around the crack tip at the onset of crack growth (r_p) is determined and added to the length of the pre-existing crack (a_0) to form a virtual crack with the length of (a_0+r_p). Then, the value of K_I is computed for the virtual crack, to which the same fracture load is applied. The result is the modified K_{IC} value, called

here K_{IC}^{*}. Equation (4) presents the Irwin's estimation of r_p, in which σ_y is the material yield strength in an elastic-perfectly plastic (EPP) material [38].

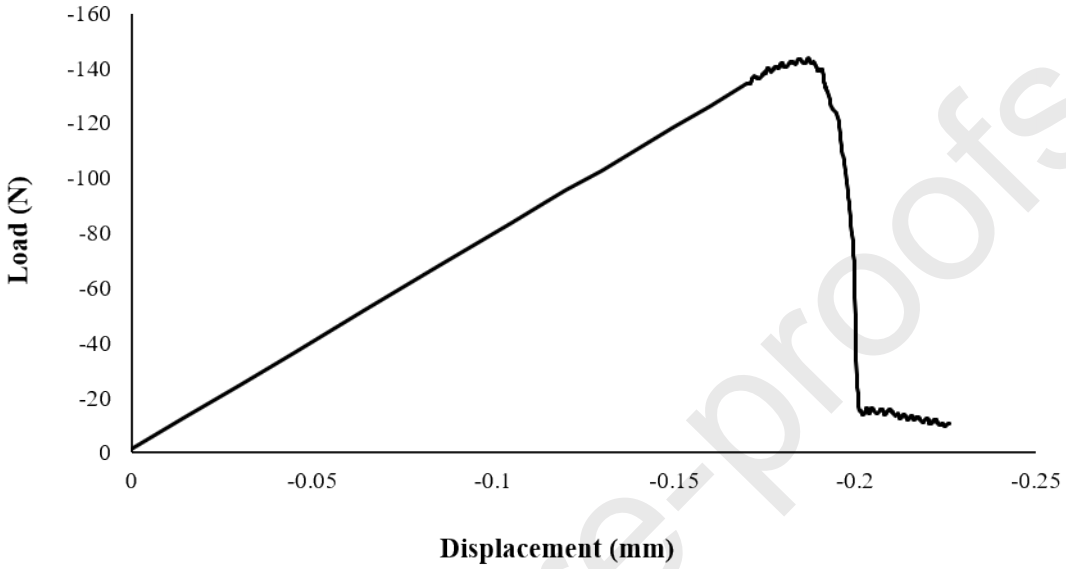

Fig. 12. A load-displacement curve for the cracked dental material specimen.

$$r_p = \frac{1}{\pi} \times \left(\frac{K_{IC}}{\sigma_y}\right)^2 \quad (4)$$

Considering that K_{IC} and σ_y for the dental material are 1.32 MPa.m$^{0.5}$ and 34.7 MPa, respectively, the value of r_p is computed to be equal to 0.46 mm. Adding 0.46 mm to the initial crack length (i.e., 8 mm, see Figure 3b) leads to a virtual crack of 8.46 mm long, for which K_{IC}^{*} is computed to be equal to 1.41 MPa.m$^{0.5}$.

Now, by substituting K_{IC} (1.32 MPa.m$^{0.5}$) and σ_u (48.7 MPa) into equations (2) and (3) instead of K_{IC} and σ_c , respectively, the values of the critical distances r_c and d_c are calculated to be approximately equal to 0.12 mm and 0.48 mm, respectively. To predict the fracture

loads of the U-notched dental material specimens by means of the classical MTS criterion (i.e., without considering the material nonlinearity), first, an arbitrary load of 100 N is applied to the FE model of the specimen and the distribution of the linear elastic tangential stress is determined on the U-notch bisector line. Then, the value of tangential stress at the distance r_c=0.12 mm from the notch tip ($\sigma_{\theta\theta}$) is obtained. Since, at the moment of fracture, the tangential stress should reach $\sigma_c = \sigma_u = 48.7$ MPa, the fracture load of the specimen (P_f) can be estimated as

$$P_f = \frac{48.7}{\sigma_{\theta\theta}} \times 100\ N \tag{5}$$

For the classical MS criterion, the procedure of the fracture load prediction is very similar to that for the MTS criterion, except that the average value of tangential stress over d_c=0.48 mm ($\overline{\sigma_{\theta\theta}}$) is used in equation (5) instead of $\sigma_{\theta\theta}$. Thus, the fracture load (P_f) estimated by MS criterion is

$$P_f = \frac{48.7}{\overline{\sigma_{\theta\theta}}} \times 100\ N \tag{6}$$

As mentioned above, the dental material has a clear nonlinear behavior (Figure 6), and the proper U-notched specimens significantly deviates from the linear-elastic behavior (Figure 7), suggesting a non-negligible plastic zone size around the notch tip. Therefore, when dealing with the prediction of fracture loads, it is intended here to consider the non-linear behavior of the U-notched specimens by means of the EMC. The procedures for predicting the fracture load (P_f) for the resulting EMC-MTS and EMC-MS criteria are very similar to those for the MTS and MS criteria, except that the values of r_c and d_c should be computed again, with the critical stress (σ_c) being the tensile strength of the equivalent material, σ_f^*. According to Figure 6, the area under the true stress-strain curve until the peak point (i.e., the

value $(SED)_D$ in equation (1)) is obtained to be equal to 1.33 MPa. Using equation (1), the value of σ_f^* results 87.4 MPa. Substituting K_{IC}^*=1.41 MPa.m$^{0.5}$ and σ_f^* = 87.4 MPa into equations (1) and (2) instead of K_{IC} and σ_c, respectively, the values of r_c and d_c for the EMC-MTS and EMC-MS criteria are computed equal to 0.04 mm and 0.16 mm, respectively. Finally, the fracture loads estimated by EMC-MTS and EMC-MS criteria are given by equations (7) and (8), in which $\sigma_{\theta\theta}$ and $\overline{\sigma_{\theta\theta}}$ (both being derived from FE analyses) are the tangential stress at r_c=0.04 mm and the average tangential stress over d_c=0.16 mm, respectively, for the arbitrary load of 100 N.

$$P_f = \frac{87.4}{\sigma_{\theta\theta}} \times 100\ N \tag{7}$$

$$P_f = \frac{87.4}{\overline{\sigma_{\theta\theta}}} \times 100\ N \tag{8}$$

5. Results and discussion

Figure 13 represents the variations of the critical loads (load-carrying capacity, LCC) of the notched dental material samples versus the notch tip radius. The figure gathers both the experimental results and the analytical predictions derived from the classical MTS and MS criteria, as well as for the combined EMC-MTS and EMC-MS criteria. As can be seen qualitatively in Figure 13, the two combined criteria are clearly more accurate than the two classical criteria, given that they take into account the material nonlinear behavior developed by the dental material samples. It is also obvious from Figure 13 that the two combined criteria are successful in predicting the experimental results, with minor differences between them, and with the EMC-MTS criterion providing predictions that are more conservative than those provided by the EMC-MS criterion. This, along with its greater simplicity, suggest that the EMC-MTS criterion could be the preferred criterion in structural engineering design.

Moreover, Table 5 summarizes the discrepancies (Δ, %) between the estimations and the (average) experimental critical loads of the U-notched dental material specimens. Negative values of the discrepancy imply underestimations of the critical loads (conservative predictions), whereas positive values are associated to overestimations of the critical loads.

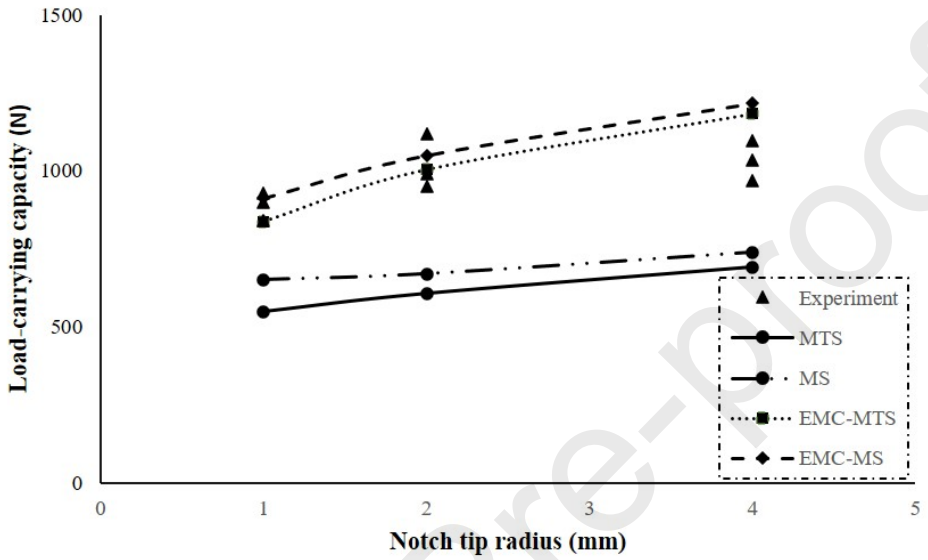

Fig. 13. Variations of the load-carrying capacity of the U-notched dental material samples versus the notch tip radius for the four theoretical criteria together with the experimental results.

Table 5. Percent discrepancies between the theoretical and experimental results (Δ).

Specimen index	Δ (%) for MTS criterion	Δ (%) for MS criterion	Δ (%) for EMC-MTS criterion	Δ (%) for EMC-MS criterion
T-1	- 38	- 27	- 6	+ 2
T-2	- 40	- 34	- 2	+ 2
T-4	- 32	- 28	+15	+18

It is evident in Table 5 that the EMC is capable of reducing the discrepancies of the MTS and MS criteria significantly, demonstrating its suitability in predicting nonlinear fracture of notched dental material specimens. Moreover, Table 5 shows that the predictions by the two combined criteria for 4 mm notch tip radius are weaker than those for 1 mm and 2 mm tip radii. To explain this issue, it should be noted that static fracture of blunt notched members can be predicted generally by means of two various approaches; (*i*) stress intensity factor (SIF) and (*ii*) stress concentration factor (SCF). The first approach is followed by the notch fracture mechanics (NFM), which is suitable for those round notches having rather small tip radii. As the notch tip radius tends towards zero (becoming a sharp crack), the stress gradient around the notch becomes higher and the accuracy of NFM enhances. The second approach, however, is useful for blunt notches with rather large tip radii for which the stress gradient in the notch vicinity is low. Those notches having moderate stress gradient might be analyzed either by the first approach or the second approach. Note that for the notched specimens tested herein, the U-notch with 4 mm tip radius has moderate stress gradient and therefore, the predictions of the two fracture criteria of NFM applied show considerable difference with the experimental results. The SCF approach is not followed herein, because the framework of the theoretical fracture predictions is based on the NFM approach.

Figure 14 shows the Von-Mises stress distributions, obtained from the elastic-plastic FE analyses, around the U-shaped notches of the dental material samples and at fracture onset (i.e., when applying the corresponding critical loads). It can be observed that the plastic zone sizes on the notch bisector line are approximately equal to 1.32, 2.13, and 2.63 mm for the notch tip radii (1, 2, and 4 mm, respectively). Considering the ligament size, which is constant and equal to 5 mm (see Figure 3a), the failure regime for 1 mm notch tip radius is recognized as the moderate-scale yielding (MSY) regime, while for the 2 and 4 mm radii it is the large-scale yielding (LSY) regime.

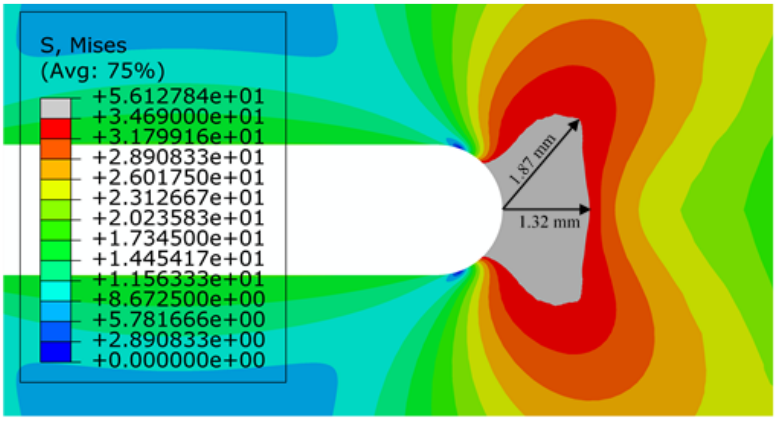

(a)

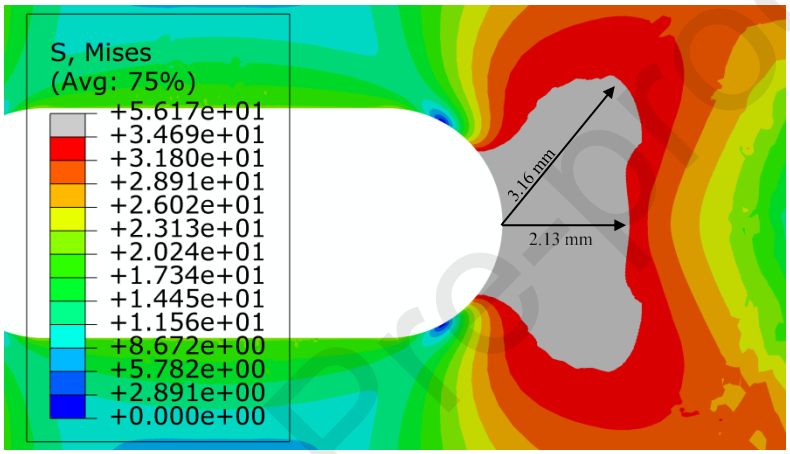

(b)

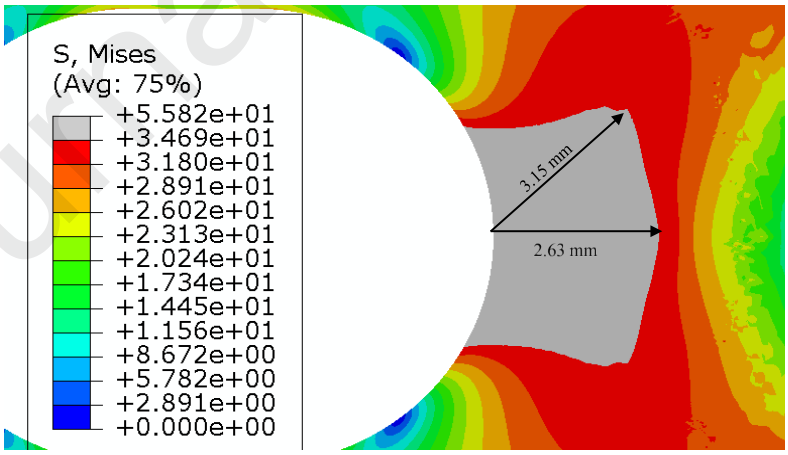

(c)

Fig. 14. Von-Mises stress distributions around U-notches in the dental material samples associated with the fracture loads: (a) notch tip radius of 1 mm, (b) 2 mm, and (c) 4 mm.

Finally, it is very useful to discuss on an important point regarding the amount of ductility of polymers being investigated for notch fracture by EMC. Note that to apply EMC, (*i*) the strain-to-failure should be small or medium (up to about 20%) according to the authors' extensive experience and (*ii*) the K-based fracture toughness (K_{IC}) should be valid, which can be realized by rather low strain-hardening of material. To the best of the authors' knowledge, no paper has been already published in open literature dealing with the fracture study in highly ductile polymers such as Polypropylene (PP) and Polyethylene (PE) etc. by EMC. But, it has been shown in several papers that the failure strain of some investigated materials reaches 20% [23, 39-42]. Moreover, in the original paper published by the first author in 2012, EMC has been shown to be effective for a type of steel with more than 50% elongation [28]. A branch of EMC, namely the Fictitious Material Concept (FMC), has also been developed to be used for those materials with large values of strain-to-failure [43, 44]. By means of FMC, it is expected that highly ductile polymers can also be successfully equated with virtual brittle materials for fracture prediction. Undoubtedly, further examinations are required to check the validity of this expectation.

5. Conclusions

The main conclusions of this research can be summarized as follows:

1. Experimental results were provided regarding the nonlinear fracture of polymeric dental material samples weakened by U-shaped notches. The load-displacement curves for the notched samples, as well as the Finite Element analyses, clearly indicated the presence of significant plastic zone in the notch vicinity at the onset of fracture.

2. Although the classical (linear-elastic) fracture criteria, e.g. the MTS and MS criteria, were easily applied for the prediction of the critical loads of the dental material notched samples, they had significant deficiencies in estimating the experimental results due to the material nonlinear behavior at the tip of the U-notches. In order to take into account the effects of the plastic zone on the final predictions, the EMC was linked to the MTS and the MS criteria. In general, it was found that the EMC-MTS and EMC-MS criteria can reduce significantly the discrepancies between the classical MTS and MS criteria and the experimental results, demonstrating the effectiveness of the EMC in the prediction of critical loads of notched polymeric dental materials with nonlinear behavior.
3. Elastic-plastic FE analyses showed that the failure regimes in the tested dental material samples were MSY for 1 mm notch tip radius and LYS for 2 and 4 mm tip radii. Therefore, in cases where the failure regime is other than the small-scale yielding (SSY), the use of the EMC in combination with MTS and MS criteria is justifiable. For the SSY regime, however, the use of the classical MTS and MS criteria should be sufficient.

Data Availability Statement

The authors declare that the data provided in the present manuscript is not confidential and is available to whom it may concern. Any additional information regarding the manuscript content will be provided on request.

References

[1] Topoleski, L. and R. Rodriguez-Pinto, *7.2 Bone Cement.* 2017.

2. Charnley, J. and J. Charnley, *Acrylic Cement in Orthopedic Surgery Baltimore.* The Williams and Wilkins Co.: Philadelphia, PA, USA, 1970: p. 36.

3. Saha, S. and S. Pal, *Mechanical properties of bone cement: a review.* Journal of biomedical materials research, 1984. **18**(4): p. 435-462.

4. Bialoblocka-Juszczyk, E., et al., *Fracture properties of an acrylic bone cement.* Acta of Bioengineering and Biomechanics, 2008. **10**(1): p. 21.

5. Khandaker, M., Y. Li, and T. Morris, *Micro and nano MgO particles for the improvement of fracture toughness of bone–cement interfaces.* journal of biomechanics, 2013. **46**(5): p. 1035-1039.

6. May-Pat, A., J. Cervantes-Uc, and S. Flores-Gallardo, *Essential work of fracture: An approach to study the fracture behavior of acrylic bone cements modified with comonomers containing amine groups.* Polymer testing, 2013. **32**(2): p. 291-298.

7. Zor, M., M. Küçük, and S. Aksoy, *Residual stress effects on fracture energies of cement–bone and cement–implant interfaces.* Biomaterials, 2002. **23**(7): p. 1595-1601.

8. Freitag, T.A. and S.L. Cannon, *Fracture characteristics of acrylic bone cements. I. Fracture toughness.* Journal of biomedical materials research, 1976. **10**(5): p. 805-828.

9. Robinson, R., T. Wright, and A. Burstein, *Mechanical properties of poly (methyl methacrylate) bone cements.* Journal of Biomedical Materials Research, 1981. **15**(2): p. 203-208.

10. Merta, I., et al., *Size and boundary effects on notch tensile strength and fracture properties of PMMA bone cement.* Polymer Testing, 2017. **59**: p. 441-448.

11. Lewis, G. and S. Mladsi, *Correlation between impact strength and fracture toughness of PMMA-based bone cements.* Biomaterials, 2000. **21**(8): p. 775-781.

12. May-Pat, A., et al., *Comparative study on the mechanical and fracture properties of acrylic bone cements prepared with monomers containing amine groups.* Journal of the mechanical behavior of biomedical materials, 2012. **6**: p. 95-105.

13. Ayatollahi, M.R., S.A. Mirmohammadi, and H.A. Shirazi, *The tension-shear fracture behavior of polymeric bone cement modified with hydroxyapatite nano-particles.* Archives of Civil and Mechanical Engineering, 2018. **18**(1): p. 50-59.

14. Gómez, F. and M. Elices, *A fracture criterion for blunted V-notched samples.* International Journal of Fracture, 2004. **127**(3): p. 239-264.

15. Ayatollahi, M.R and A.R Torabi, *Determination of mode II fracture toughness for U-shaped notches using Brazilian disc specimen.* International Journal of Solids and Structures, 2010. **47**(3-4): p. 454-465.

16. Ayatollahi, M.R and A.R Torabi, *A criterion for brittle fracture in U-notched components under mixed mode loading.* Engineering Fracture Mechanics, 2009. **76**(12): p. 1883-1896.

17. Ayatollahi, M.R and A.R Torabi, *Investigation of mixed mode brittle fracture in rounded-tip V-notched components.* Engineering Fracture Mechanics, 2010. **77**(16): p. 3087-3104.

18. Gómez, F., et al., *Fracture of U-notched specimens under mixed mode: experimental results and numerical predictions.* Engineering Fracture Mechanics, 2009. **76**(2): p. 236-249.

19. Zhou, J., Y. Wang, and Y. Xia, *Mode-I fracture toughness measurement of PMMA with the Brazilian disk test.* Journal of materials science, 2006. **41**(17): p. 5778-5781.

20. Bura, E. and A. Seweryn, *Mode I fracture in PMMA specimens with notches–Experimental and numerical studies.* Theoretical and Applied Fracture Mechanics, 2018. **97**: p. 140-155.

21. Ayatollahi, M.R, M. Aliha, and M. Hassani, *Mixed mode brittle fracture in PMMA—an experimental study using SCB specimens.* Materials Science and Engineering: A, 2006. **417**(1-2): p. 348-356.

22. Ayatollahi, M.R and A.R Torabi, *Brittle fracture in rounded-tip V-shaped notches.* Materials & Design, 2010. **31**(1): p. 60-67.

23. Torabi, A.R, A. Rahimi, and M.R Ayatollahi, *Tensile fracture analysis of a ductile polymeric material weakened by U-notches.* Polymer Testing, 2017. **64**: p. 117-126.

24. Akbardoost, J., et al., *Scaling effect on the fracture toughness of bone materials using MMTS criterion.* Journal of the mechanical behavior of biomedical materials, 2018. **85**: p. 72-79.

25. Taylor, D., et al., *The effect of stress concentrations on the fracture strength of polymethylmethacrylate.* Materials Science and Engineering: A, 2004. **382**(1-2): p. 288-294.

26. Karimzadeh, A. and M.R Ayatollahi, *Investigation of mechanical and tribological properties of bone cement by nano-indentation and nano-scratch experiments.* Polymer Testing, 2012. **31**(6): p. 828-833.

27. Standard, A., *D638: Standard test method for tensile properties of plastics.* West Conshohocken (PA): ASTM International, 2010.

28. Torabi, A.R., *Estimation of tensile load-bearing capacity of ductile metallic materials weakened by a V-notch: The equivalent material concept.* Materials Science and Engineering: A, 2012. **536**: p. 249-255.

29. Erdogan, F. and G. Sih, *On the crack extension in plates under plane loading and transverse shear.* 1963.

30. Torabi, A.R, A. Campagnolo, and F. Berto, *Local strain energy density to predict mode II brittle fracture in Brazilian disk specimens weakened by V-notches with end holes.* Materials & design, 2015. **69**: p. 22-29.

31. Torabi, A.R and F. Berto, *Notch fracture toughness evaluation for a brittle graphite material.* Materials Performance and Characterization, 2014. **3**(3): p. 398-413.

32. Torabi, A.R, A. Campagnolo, and F. Berto, *Mode II brittle fracture assessment of key-hole notches by means of the local energy.* Journal of Testing and Evaluation, 2016. **44**(3): p. 1261-1270.

33. Rodriguez, J., et al., *Fracture of notched samples in epoxy resin: Experiments and cohesive model.* Engineering Fracture Mechanics, 2015. **149**: p. 402-411.

34. Kinloch, A. and J. Williams, *Crack blunting mechanisms in polymers.* Journal of Materials Science, 1980. **15**(4): p. 987-996.

35. Tsuji, K., K. Iwase, and K. Ando, *An investigation into the location of crack initiation sites in alumina, polycarbonate and mild steel.* Fatigue & fracture of engineering materials & structures (Print), 1999. **22**(6): p. 509-517.

36. Torabi, A.R, *Fracture assessment of U-notched graphite plates under tension.* International Journal of Fracture, 2013. **181**(2): p. 285-292.

37. Anderson, T.L., *Fracture mechanics: fundamentals and applications*. 2017: CRC press.

38. Irwin, G., *Plastic zone near a crack and fracture toughness.* 1997.

39. Berto, F. and S.M.J. Razavi, *Ductile failure prediction of thin notched aluminum plates subjected to combined tension-shear loading.* 2018.

40. Torabi, A.R, F. Berto, and S.M.J. Razavi, *Tensile failure prediction of U-notched plates under moderate-scale and large-scale yielding regimes.* Theoretical and Applied Fracture Mechanics, 2018. **97**: p. 434-439.

41. Majidi, H., A.R Torabi, and M. Golmakani, *J-integral expression for mixed mode I/II ductile failure prediction of U-notched Al 6061-T6 plates under large-scale yielding regime.* Engineering Fracture Mechanics, 2018. **195**: p. 253-266.

42. Rahimi, A., M.R Ayatollahi, and A.R Torabi, *Fracture study in notched ductile polymeric plates subjected to mixed mode I/II loading: Application of equivalent material concept.* European Journal of Mechanics-A/Solids, 2018. **70**: p. 37-43.

43. Torabi, A.R., Kamyab, M., *The fictitious material concept.* Engineering Fracture Mechanics, 2019. **209**: p. 17-31.

44. Torabi, A.R., Kamyab, M., *Mixed mode I/II failure prediction of thin U-notched ductile steel plates with significant strain-hardening and large strain-to-failure: the Fictitious Material Concept.* European Journal of Mechanics-A/Solids, 2019. **75**: p. 225-236.

Highlights:

- Nonlinear fracture analysis of U-notched specimens made of biopolymer is performed.
- Tensile biopolymer samples with internal U-notches are tested under mode I loading.
- Equivalent Material Concept is used to change elastoplastic domain to elastic one.
- EMC is combined with MTS and MS criteria to estimate the critical loads of samples.
- Both EMC-MTS/MS models are successful in fracture prediction of biopolymer samples.

CRediT authorship contribution statement

A.R. Torabi: Conceptualization, Methodology, Supervision, Writing – review & editing. **Sahel Shahbaz:** Software, Writing – original draft, Visualization, Investigation, Validation, Data curation. **S. Cicero:** Conceptualization, Writing – review & editing. **M.R. Ayatollahi:** Project administration, Supervision, Writing – review & editing.

Declaration of interests

The authors declare that they have no known competing financial interests or personal relationships that could have appeared to influence the work reported in this paper.